Drug Design, Development and Therapy

Dovepress
open access to scientific and medical research

Open Access Full Text Article

ORIGINAL RESEARCH

Enhancement of Antitumor Efficacy of Paclitaxel-Loaded PEGylated Liposomes by N, N-Dimethyl Tertiary Amino Moiety in Pancreatic Cancer

This article was published in the following Dove Press journal:
Drug Design, Development and Therapy

Yang Chen[1,*]
Li Wang[1,*]
Shi Luo[2]
Jun Hu[3]
Xing Huang[1]
Pei-Wen Li[2]
Yi Zhang[1]
Chao Wu[1]
Bo-Le Tian[1]

[1]Department of Pancreatic Surgery, West China Hospital of Sichuan University, Chengdu 610041, Sichuan Province, People's Republic of China; [2]Key Laboratory of Drug Targeting and Drug Delivery Systems, Ministry of Education, West China School of Pharmacy, Sichuan University, Chengdu 610041, People's Republic of China; [3]Laboratory of Basic Scientific Research, West China Hospital of Sichuan University, Chengdu 610041, Sichuan Province, People's Republic of China

*These authors contributed equally to this work

Introduction: Pancreatic cancer, or pancreatic duct adenocarcinoma (PDAC), remains one of the most lethal cancers and features insidious onset, highly aggressive behavior and early distant metastasis. The dense fibrotic stroma surrounding tumor cells is thought to be a shield to resist the permeation of chemotherapy drugs in the treatment of PDAC. Thus, we synthesized a pancreas-targeting paclitaxel-loaded PEGylated liposome and investigated its antitumor efficacy in the patient-derived orthotopic xenograft (PDOX) nude mouse models of PDAC.

Methods: The PTX-loaded PEGylated liposomes were prepared by film dispersion-ultrasonic method and modified by an N,N-dimethyl tertiary amino residue. Morphology characteristics of the PTX-loaded liposomes were observed by transmission electron microscope (TEM). The PDOX models of PDAC were established by orthotopic implantation and imaged by a micro positron emission tomography/computed tomography (PET/CT) imaging system. The in vivo distribution and antitumor study were then carried out to observe the pancreas-targeting accumulation and the antitumor efficacy of the proposed PTX liposomes.

Results: PTX loaded well into both modified (PTX-Lip2N) and unmodified (PTX-Lip) PEGylated liposomes with spherical shapes and suitable parameters for the endocytosis process. The PDOX nude mouse models were successfully created in which high ^{18}F-FDG intaking regions were observed by micro-PET/CT. In addition to higher cellular uptakes of PTX-Lip2N by the BxPC-3 cells, the proposed nanoparticle had a notable penetrating ability towards PDAC tumor tissues, and consequently, the antitumor ability of PTX-Lip2N was significantly superior to the unmodified PTX-Lip in vivo PDOX models and even more effective than nab-PTX in restraining tumor growth.

Conclusion: The modified pancreas-targeting PTX-loaded PEGylated liposomes provide a promising platform for the treatment of pancreatic cancer.

Keywords: pancreas-targeting, tertiary amine, pancreatic duct adenocarcinoma, paclitaxel liposome, antitumor efficacy

Correspondence: Bo-Le Tian
Department of Pancreatic Surgery, West China Hospital of Sichuan University, No. 37 Guo Xue Road, Chengdu, Sichuan Province 610041, People's Republic of China
Tel +86 13880683475
Fax +86 28-85422475
Email tianbolemed@163.com

Introduction

Currently, pancreatic cancer is gradually becoming a fatal digestive system carcinoma throughout the world with a rising trend in morbidity and a persistent high level of mortality that is estimated to be the fourth leading cause of cancer-related death.[1] The major pathological type of pancreatic cancer is pancreatic duct

submit your manuscript | www.dovepress.com
DovePress
http://doi.org/10.2147/DDDT.S261017

adenocarcinoma (PDAC), which accounts for over 90% of cases and features insidious onset, highly aggressive behavior and early distant metastasis.[2,3]

Although radical resection followed by adjuvant chemotherapy is the only potentially curative treatment of PDAC, less than one-fifth of patients with PDAC could meet the essential surgical standard once diagnosed and subsequently undergo surgical resections, most of which would suffer from recurrent conditions with locally advanced tumor or distant metastasis within a year.[4–6] Given that, numerous therapeutic strategies, including chemotherapy, radiotherapy, targeted therapy, etc., in addition to surgical treatment have been carried out in this field. However, only a few regimens based on cytotoxic drugs have improved the outcomes of patients with PDAC to some extent.[7–11] The current guidelines still recommend gemcitabine, since the late 1990s, plus nanomolecular albumin-bound paclitaxel (nab-PTX) or FOLFIRINOX, a quadruple regimen of 5-fluorouracil, leucovorin, irinotecan and oxaliplatin, as the first-line chemotherapy to deal with this devastating disease if it is unresectable.[3,12] Despite notable progress that has been achieved in detecting procedure and comprehensive therapy of PDAC, the poor prognosis is still frustrating, with a persistently low 5-year survival rate of 6–9%.[13,14]

Both the invasive nature with early recurrence and metastasis and the development of chemical resistance can contribute in part to the poor prognosis of PDAC.[15,16] To date, the dense fibro-inflammatory stroma that develops along with the tumor cells has been highlighted as a shield to resist the permeation of chemotherapy drugs.[17] Formulations that target or inhibit tumor stroma or with high-penetrating ability towards tumor tissue have been reported to improve survival outcomes.[18,19] For example, nab-PTX, which is aimed at overexpressing albumin-binding protein in PDAC stroma, has successfully attained a high intratumoral concentration of the drug and offered significant antitumor properties when in combination with gemcitabine.[20] Thus, an appropriate nanomolecular delivery system carrying chemotherapeutic drugs with high efficiency to penetrate the barrier of the tumor stroma would be a promising strategy to improve the prognosis of PDAC.

In our previous studies, a series of derivatives of HIPDM (N,N,N'-trimethyl-N'-(2-hydroxy-3-methyl-5-iodobenzyl)-1,3-propane diamine), a brain perfusion imaging agent with a notable affinity for the pancreas,[21,22] were constructed in conjugation with several crude drugs, in which the structure of the propanediamine moiety with a tertiary amine, eg, N,N-dimethyl-ethanolamine or N,N-dimethyl-1,2-diaminoethane, presents a notable pancreatic targeting ability.[23,24] The Pancreas and brain have both been reported to have acidic microenvironments.[25,26] Thus, the proposed mechanism of this phenomenon may be associated with the pH gradient between the acidic microenvironment of the pancreas and relatively alkaline plasm where the conjugated tertiary amine moiety could exhibit a notable affinity for the pancreas and cross the epithelial barrier between the blood and pancreas, named blood–pancreas barrier (BPB),[27,28] to mediate the targeted accumulation in the pancreas.

Based on these findings, we synthesized a novel PEGylated liposome in our previous research modified by DSPE-PEG_{2000}-2N, a new compound with an amido linkage between N,N-dimethyl-1,3-propanediamine and 1.2-distearoyl-sn-glycero-3-phosphoethanolamine-N-[succinimidyl (polyethylene glycol)-2000] (DSPE-PEG_{2000}-NHS), outside the membrane and preliminarily examined its drug delivery efficiency towards the pancreas.[29] However, the penetrating ability of this nanoparticulate delivery system and the concentration of loaded drug into PDAC tumor tissues are still unknown. In the current study, we conducted a further experiment by loading PTX in patient-derived orthotopic xenograft (PDOX) nude mouse models to determine whether this new drug delivery system targeting the pancreas could improve the therapeutic efficacy of PTX against PDAC.

Materials and Methods

Materials

PTX and nab-PTX were both purchased from Hengrui Pharmaceutical Co., Ltd (Shanghai, CN). 1.2-Distearoyl-sn-glycero-3-phosphoethanolamine-N-methoxy (polyethylene glycol)-2000 (mDSPE-PEG_{2000}) was purchased from Laysan Bio, Inc (Hawaii, USA). The modified ligand DSPE-PEG_{2000}-2N was synthesized in the National Laboratory of West China Pharmaceutical School of Sichuan University as described previously.[29] 1,1′-Dioctadecyl -3,3,3′,3′-tetramethylindodicarbocyanine perchlorate (DiD) was obtained from Best Reagent Co., Ltd (Chengdu, CN). All other chemicals were of analytical or high-performance liquid chromatography grade.

Animals and Cell Cultures

Athymic BALB/c-nu/nu male nude mice and NOD/SCID male mice (GemPharmatech Co., Ltd., Jiangsu, CN), both

4–6 weeks old, were used to construct the PDOX models. The mice were maintained in the individual ventilated cages (IVC) of a specific pathogen free (SPF) facility under standard conditions with 12-h light-dark cycles and allowed free access to food and water throughout the entire experiment. All animal experiments were performed in accordance with the guidelines approved by the Institutional Animal Care and Ethics Committee of Sichuan University (approval no. 2019198A).

BxPC-3 cells (a human pancreatic adenocarcinoma cell line) were obtained from the ATCC (Virginia, USA), cultured in RPMI-1640 (GIBCO, USA) supplemented with 10% fetal bovine serum (GIBCO, USA) and 100 U/mL penicillin/streptomycin that was changed every two days and incubated at 37°C in a humidified atmosphere containing 5% CO_2.

Preparation of Liposomes

The PTX-loaded PEGylated liposomes were prepared by the film dispersion-ultrasonic method. First, chloroform solutions of LipoidS100 (20 mg/mL), cholesterol (10 mg/mL), mDSPE-PEG_{2000} (5 mg/mL), DSPE-PEG_{2000}-2N (2 mg/mL) and PTX (1 mg/mL) were prepared and stored. After taking the above solutions at a volume ratio of 1:1:0.8:0.5:1, respectively, and mixing them in an empty flask, the solvent of the mixture was removed under negative pressure in a rotary evaporator at 37°C for over 10 min to form a uniform transparent film. Finally, adequate phosphate-buffered saline (PBS) was added to the flask according to the final concentration needed to hydrate the adherent film at room temperature for 20 min and then an ultrasonic cell crasher was utilized to sonicate the suspension for 8 min at 100 W (3 s pulse and 5 s rest) to acquire the modified liposomes containing PTX (PTX-Lip2N). Unmodified PTX liposomes (PTX-Lips) were prepared with LipoidS100, cholesterol, mDSPE-PEG_{2000} and PTX stored previously at a volume ratio of 1:1:1:1 by the film dispersion-ultrasonic method mentioned above. DiD-labeled liposomes (DiD-Lip/DiD-Lip2N) were prepared by using a chloroform solution of DiD instead of PTX according to the same procedure.

Characterization

The morphology characteristics of PTX-loaded liposomes were observed by transmission electron microscope (TEM, H-600, Hitachi, Tokyo, Japan). A droplet of suspension solution (0.5 mg/mL) was deposited on a copper grid covered with nitrocellulose, negatively stained with phosphotungstic acid, and allowed to dry at room temperature before TEM observation. The particle size and polydispersity index (PDI) of PTX-Lip/PTX-Lip2N were determined by dynamic light scattering using a Malvern Zetasizer NanoZS90 (Malvern Instruments, Malvern, UK). All experiments were repeated three times.

The content of PTX encapsulated in PTX-Lip/PTX-Lip2N was determined by the membrane filter method. The encapsulation efficiency (EE) and drug-loading (DL) coefficient were calculated according to following formulas:[30]

EE%= (weight of drug loaded/weight of drug fed) ×100%

DL%= (weight of drug loaded/total weight of materials added) ×100%.

In vitro Cellular Uptake

Cellular uptake of the PTX-Lip2N/PTX-Lip was quantitatively measured by using DiD as a fluorescent probe instead of PTX loaded in the liposomes.[31,32] Briefly, BxPC-3 cells were cultured in a 12-well plate at a density of 1×10^5 cells per well and incubated for 24 h at 37°C in a humidified atmosphere containing 5% CO_2. After that, serum-free culture media containing free DiD, DiD-Lip and DiD-Lip2N with the same final DiD concentration of 0.5 μg/mL were applied to replace the original medium and incubated at 37°C.

Fluorescence imaging experiments were performed on an A1RMP two-photon confocal laser scanning microscope (Nikon, Japan). After incubation, each well was washed with cold PBS three times to eliminate residual DiD, and then the cells were fixed with 4% paraformaldehyde for 15 min at room temperature. A blue fluorescent stain, 4′,6-diamidino-2-phenylindole (DAPI), was used to stain the cell nucleus before the final fluorescence imaging.

The fluorescence intensity of the cells was evaluated by a FACSVerse flow cytometer (BD, USA). After incubation, the cells were harvested using 0.25% trypsin-EDTA, washed twice with cold PBS, and finally resuspended in 0.5 mL of PBS for flow-cytometry measurements.

Cell Proliferation Assay

The cytotoxicities of PTX, PTX-Lip, PTX-Lip2N and nab-PTX were evaluated by MTT assay in BxPC-3 cells. Briefly, cells were plated in 96-well plates at a density of 1×10^4 cells/well and incubated in a 5% CO_2 atmosphere at 37 °C for 24 h before intervention. Subsequently, the cells were

treated with a series of twofold dilutions of PTX from the above preparations for 48 h. Cells were then incubated with 20 μL of MTT (5 mg/mL in PBS) for another 4 h and the formed crystals were dissolved in 150 μL of DMSO per well. The absorbance at 570 nm was measured using a microplate reader (Bio-Rad, USA). The cell viability (%) was calculated using the following formula:

$$\text{Cell viability (\%)} = (A_{[Test]}\text{-}A_{[Blank]})/(A_{[Control]}\text{-}A_{[Blank]}) \times 100\%$$

where $A_{[Test]}$, $A_{[Control]}$, and $A_{[Blank]}$ represent the absorbances of the treatment group, untreated control group and blank culture media group, respectively.

Establishment of PDOX Models of PDAC by Orthotopic Implantation

The PDAC tumor was acquired from a patient receiving pancreatic resection after diagnosis by fine needle aspiration biopsy under the guidance of endoscopic ultrasonography in the Department of Pancreatic Surgery, West China Hospital. Written informed consent was preciously obtained from the patient, and the Institutional Review Board of the hospital also approved this experiment.

The PDOX models of PDAC were established as described previously.[33–35] Once acquired from the specimen, the tumor was cut into fragments of approximately $3mm^3$ to transplant subcutaneously into NOD/SCID mice as the first generation. Then, the nude mice were implanted with the patient tumor growing in NOD/SCID mice as the second generation to establish the models. In brief, after anesthetization with 2.5% sodium pentobarbital (50 mg/kg, i.p.), each mouse subsequently underwent a sterile laparotomy with a 1 cm transverse incision through the skin and peritoneum under the left costal margin to expose the tail of the pancreas. The tumor fragments were implanted into the capsule of the pancreas with an inoculating needle (2 mm in diameter) and fixed with absorbable 6–0 polyglactin sutures (6–0 Vicryl, Ethicon, Inc., USA).

A micro animal positron emission tomography/computed tomography (PET/CT) imaging system (Inviscan SAS, FR) was used to confirm the establishment of the PDOX models before treatment at the Nuclear Medical Center of West China Hospital. ^{18}F- fluorodeoxyglucose (^{18}F-FDG) was used as the radioactive tracer (120 ± 10 μCi, i.v.) in this procedure.

In vivo Distribution of PTX-Lip/PTX-Lip2N in Tumor-Bearing Mice

The in vivo physiological distribution of Lip2N has already been described in our previous research. Hence, further observations of the biodistribution in normal mice at 2 h, 6 h and 24 h were carried out. In addition, we used PDOX and subcutaneous xenograft models of PDAC to detect the distribution in tumor tissues. DiD-labeled DiD-Lip and DiD-Lip2N were injected intravenously into the tail veins of the model mice at a DiD equivalent dose of 200 μg/kg. The major organs, including heart, lungs, spleen, kidneys, liver, pancreas and tumor tissue, were obtained 2 h after injection and imaged by an in vivo imaging system (IVIS, Caliper Life Sciences, USA) to determine the fluorescence intensity.[36]

In vivo Antitumor Study in the PDOX Model of PDAC

The nude mice with the PDOX model were first randomized into five treatment groups: normal saline (NS) as a control, PTX, PTX-Lip, PTX-Lip2N and nab-PTX. The drugs were injected i.v. twice a week at an equivalent dose of 5 mg/kg PTX per dose for 4 weeks. The treatment procedure began when the PDOX tumors reached $100mm^3$. Mice were sacrificed after complete treatment to harvest the tumors. Tumor volume was calculated by the following formula:

$$\text{Tumor volume} = 0.5 \times (\text{major diameter}) \times (\text{minor diameter})^2.$$

Tumor tissues were fixed in 4% paraformaldehyde and then embedded in paraffin for hematoxylin and eosin (H&E) staining and immunohistochemistry (IHC) analysis of the antigen Ki-67.[37,38] The cell proliferation rates were evaluated by the percentage of Ki-67 positive cells among total cells counted in 5 random 20 × fields.

Statistical Analysis

Statistical analyses were performed using GraphPad Prism 8.0 software. All data from the experiments are expressed as mean ± standard deviation (SD) and analyzed by Student's *t*-test or one-way analysis of variance followed by Tukey's test. A p-value of < 0.05 was considered statistically significant for all comparisons.

Results

Characterization

The microstructural schematic diagram of PTX-loaded PEGylated liposomes modified by N,

N-dimethyl-1,3-propanediamine (PTX-Lip2N) is shown in Figure 1A. The spherical lipid bilayer structures of PTX-Lip and PTX-Lip2N were observed by TEM (Figure 1B and C), and both had diameters of nearly 150 nm. The characteristics of the liposomal formulations are summarized in Table 1. The surface potentials of PTX-Lip/PTX-Lip2N were −13.8±1.3 mV and −10.1 ±1.7 mV, respectively. The average diameters of the two PTX-loaded liposomes were significantly larger than those of the two empty liposomes due to PTX introduction in the liposomal bilayer ($p < 0.05$). The PDI values were all less than 0.2, showing that these liposomes all had monodisperse systems. Finally, the encapsulation efficiencies of PTX obtained in both formulations were over 90%, and the drug-loading rates were 2.56% and 2.61%, respectively.

In vitro Cellular Uptake

Cellular internalization of free DiD, DiD-Lip and DiD-Lip2N by BxPC-3 cells was observed and imaged by confocal laser scanning microscopy (Figure 2A–C), in which more intense-red fluorescence was observed in the cytoplasmic region of the DiD-Lip2N group than in the other groups. Further study of quantitative cellular uptake by flow cytometry was consistent with the above outcomes (Figure 2D). The cellular uptake values of DiD-Lip and DiD-Lip2N were 4.07 times higher ($p < 0.05$) and 7.12 times higher ($p < 0.01$) than that of free DiD, respectively, indicating that the liposomal formulations could be more efficient in delivering PTX into pancreatic cancers. Higher uptake of DiD-Lip2N than DiD-Lip was calculated, though, without significant difference (P=0.069).

Cell Proliferation Assay

The anti-proliferative effect of PTX-Lip2N compared to free PTX, PTX-Lip or nab-PTX was determined by MTT assay in BxPC-3 cells (Figure 3). The half-maximal inhibitory concentrations (IC50s) of free PTX, PTX-Lip, PTX-Lip2N and nab-PTX were over 50 nM, 33.40 nM, 20.36 nM and 29.53 nM, respectively, against BxPC-3 cells. The other three PTX formulations all showed significant reductions in cell viability compared with free PTX ($p < 0.05$). After modification

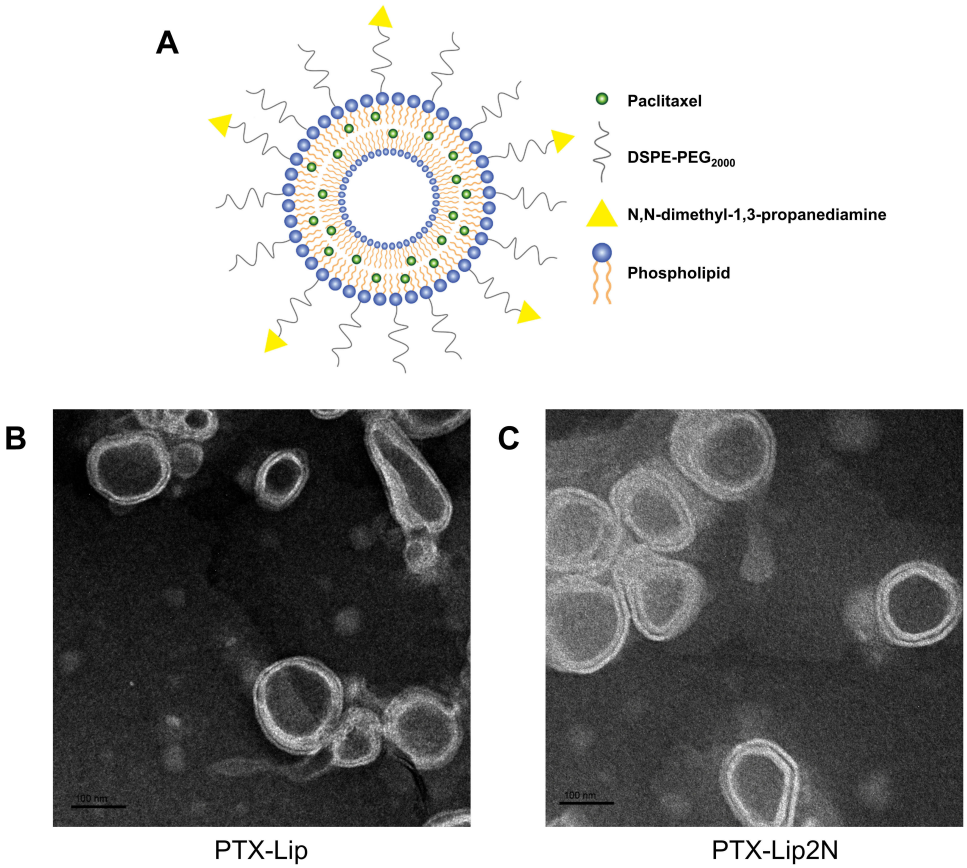

Figure 1 Microstructural schematic diagram of PTX-Lip2N (**A**), and transmission electron microscopic images of PTX-Lip (**B**) and PTX-Lip2N (**C**).

Table 1 Characterization of Liposomes (n=3, Mean± SD)

Formulation	Size (nm)	PDI ± SD	Zeta Potential (mV)	EE (%)	DL (%)
Empty Lip	126.3 ± 9.5	0.162 ± 0.11	−14.6 ± 1.9		
Empty Lip2N	129.2 ± 7.4	0.177 ± 0.07	−10.7 ± 1.6		
PTX-Lip	156.3 ± 8.2	0.192 ± 0.08	−13.8 ± 1.3	92.2 ± 2.5	2.56± 0.13
PTX-Lip2N	153.4 ± 6.4	0.183 ± 0.13	−10.1 ± 1.7	93.5 ± 3.9	2.61± 0.19

Abbreviations: PDI, polydispersity index; EE, encapsulation efficiency; DL, drug loading; PTX, paclitaxel.

by the tertiary amine derivate, N, N-dimethyl-1,3-propanediamine, PTX-Lip2N exhibited increased cytotoxicity than unmodified PTX-Lip ($p < 0.05$) and was slightly more effective than nab-PTX but without a significant difference.

In vivo Distribution Study in Tumor Tissue

Normal mice and PDOX/subcutaneous xenograft models were utilized to analyze the in vivo distribution of DiD-labeled DiD-Lip/DiD-Lip2N. Fluorescence imaging was first performed in normal mice at 2, 6 and 24 h after i.v. injections as shown in Figure 4A, and the mean fluorescent intakes of the pancreas are compared in Figure 4B. Among all three time-related groups, DiD-Lip2N showed an increased accumulation in the pancreas that was significantly higher than that of DiD-Lip. In addition, in vivo fluorescence imaging of the orthotopic/subcutaneous models is shown in Figure 5A, and the mean fluorescent intakes of the tumor tissues are compared in Figure 5B. A significantly greater fluorescence intensity was observed in the DiD-Lip2N group compared with the DiD-Lip group from the orthotopic tumor ($p < 0.05$). The fluorescent distribution of the two groups from the subcutaneous model, however, did not show any significant difference, indicating that Lip2N modified by the proposed tertiary amine derivative had an efficient penetrating ability towards PDAC tumor tissue in addition to its significant pancreas-specific accumulation.

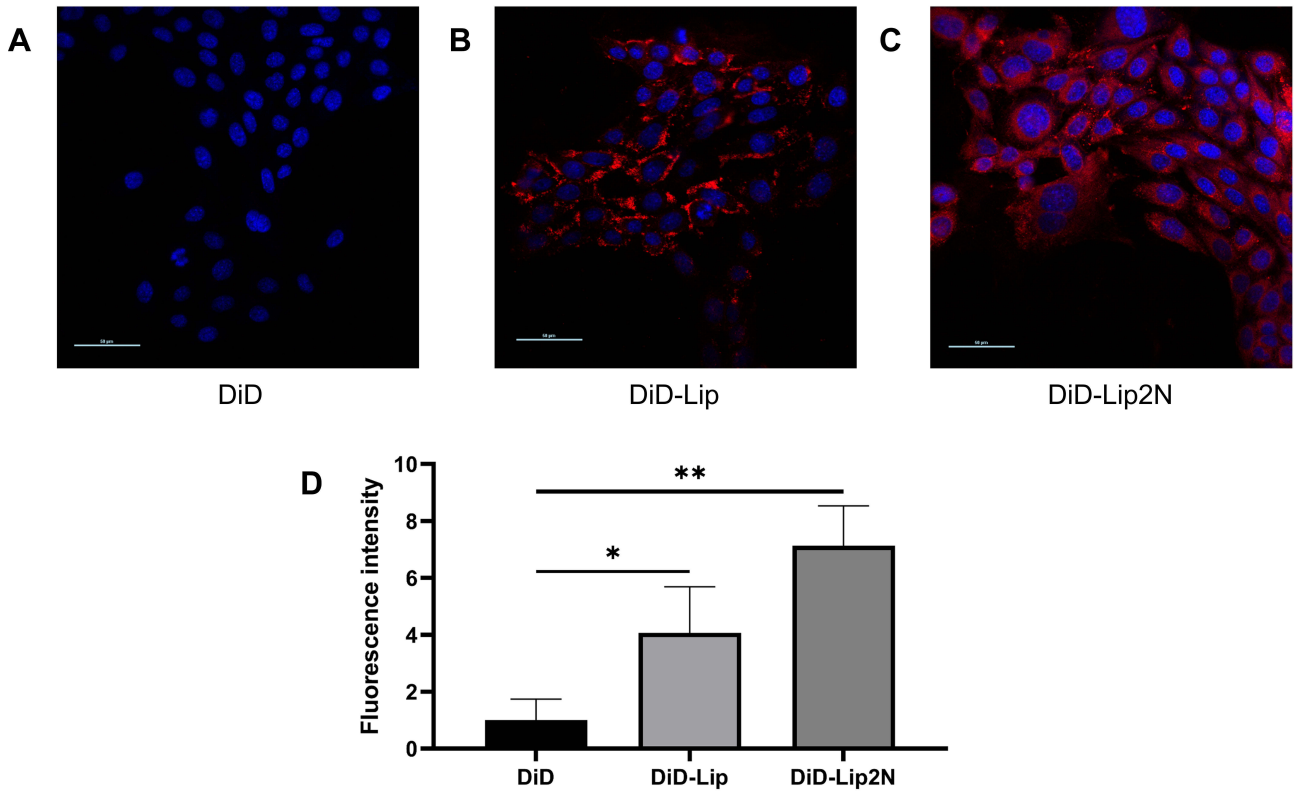

Figure 2 Confocal fluorescence images of cellular uptake by BxPC-3 cells of free DiD (**A**), DiD-Lip (**B**) and DiD-Lip2N (**C**). Scale bar, 50 μm. Mean fluorescence intensities (**D**) evaluated by flow cytometry. *$p < 0.05$, **$p < 0.01$, DiD-Lip/DiD-Lip2N versus free DiD. (n=3).

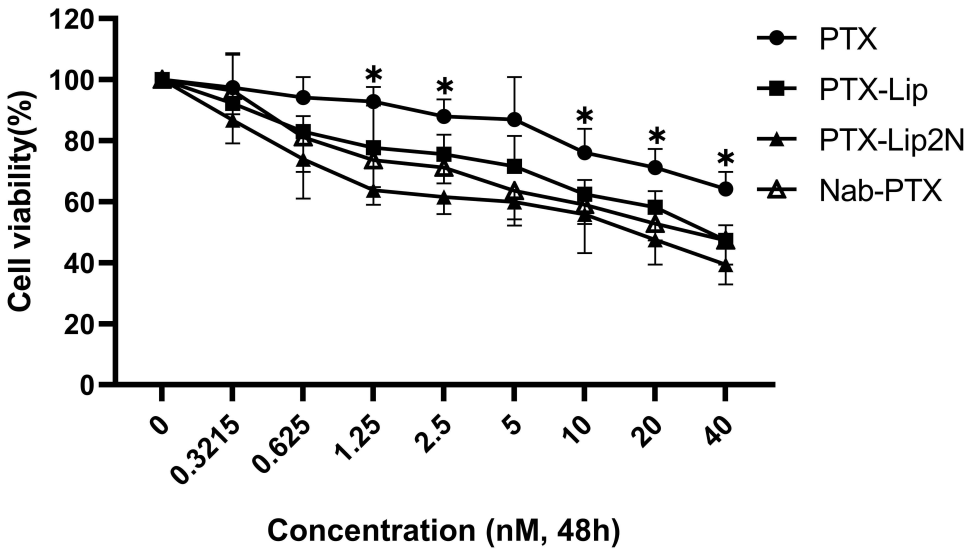

Figure 3 In vitro cytotoxicity study of different PTX formulations in BxPC-3 cells by MTT assay. *p < 0.05, versus free PTX. (n=6).

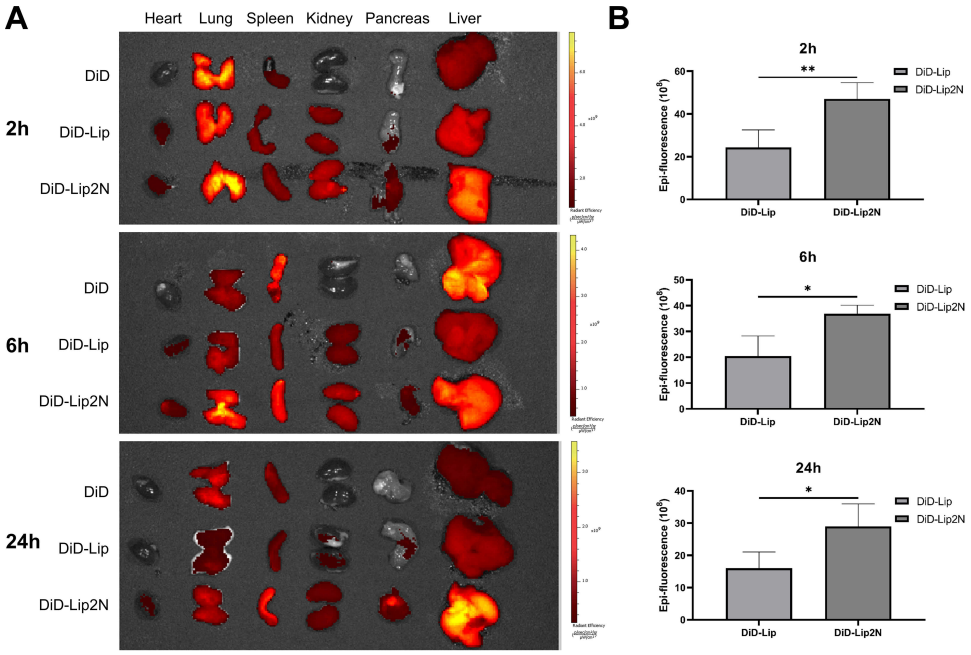

Figure 4 IVIS images of the in vivo distribution of DiD, DiD-labeled DiD-Lip/DiD-Lip2N in normal mice 2, 6 and 24 h after i.v. administration (**A**), and mean fluorescence intensities of time-related biodistributions (**B**). *p < 0.05, **p < 0.01, DiD-Lip2N versus DiD-Lip.

In vivo Antitumor Study

The ^{18}F-FDG image of the PDOX nude mouse model of PDAC by PET/CT is shown in Figure 6. The high ^{18}F-FDG intake region (marked by arrows) located in the area of the mouse pancreas was observed to confirm the successful establishment of the PDOX model. The mean tumor-to-muscle and tumor-to-blood ratios of the standardized uptake values (SUVs) of ^{18}F-FDG in the PDOX models were 1.87 ± 0.53 and 1.19 ± 0.32, respectively.

Next, sequential i.v. antitumor therapy by NS, PTX, PTX-Lip, PTX-Lip2N and nab-PTX was performed as described above. The tumor tissue specimens in the tail of the pancreas were harvested and photographed (Figure 7A), and the mean volumes of these tumors are shown in Figure 7B. The PTX (0.221 ± 0.036 cm^3) and PTX-Lip (0.184 ± 0.036 cm^3) treatment groups were both superior to the control group (0.331 ± 0.043 cm^3, $p < 0.01$) with significant antitumor efficiencies. The modified PTX-Lip2N (0.129 ± 0.022 cm^3) significantly

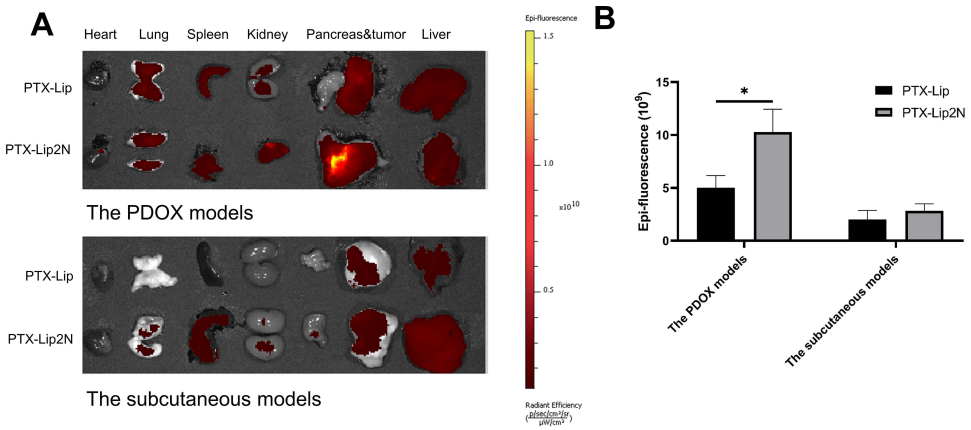

Figure 5 IVIS images of the in vivo distribution of DiD-labeled DiD-Lip/DiD-Lip2N in the PDOX/subcutaneous models of PDAC (**A**), and mean fluorescence intensity of tumor biodistributions (**B**). *p < 0.05, DiD-Lip2N versus DiD-Lip. (n=3).

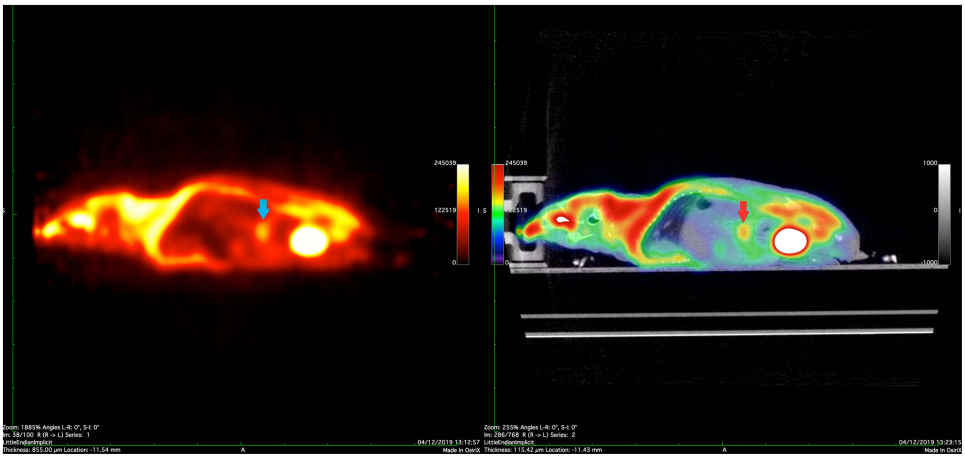

Figure 6 ^{18}F-FDG uptake of the PDOX model with PDAC by micro-PET/CT. The high ^{18}F-FDG intake region (marked by arrows) located in the area of the mouse pancreas was observed to evaluate the establishment of the PDOX model.

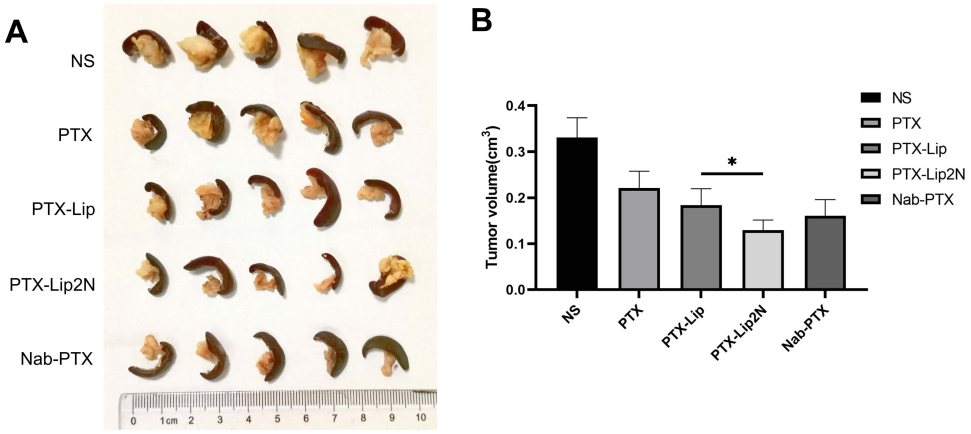

Figure 7 In vivo antitumor effects of PTX, PTX-Lip, PTX-Lip2N and nab-PTX in PDOX models of PDAC. The tumor specimens in the tail of the pancreas (**A**) and mean tumor volumes of each group at the end of the experiment (**B**). *p < 0.05, PTX-Lip2N versus PTX-Lip. (n=5).

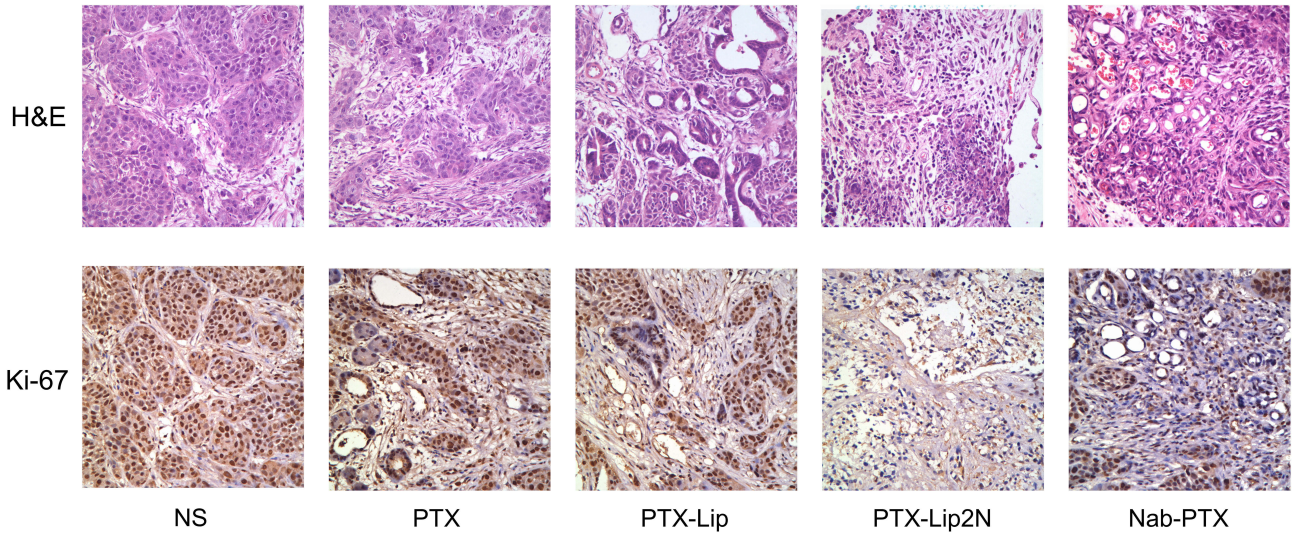

Figure 8 Representative tissue photomicrographs (H&E and antigen Ki-67 stain) from control group and treatment groups by PTX, PTX-Lip, PTX-Lip2N and nab-PTX. Magnification, 400×.

inhibited tumor growth to a greater extent than PTX-Lip ($p < 0.05$), and was slightly superior to nab-PTX (0.157 ± 0.023 cm^3, $p = 0.08$), although, there was no significant difference.

Tumor histology stained by H&E and IHC analysis of antigen Ki-67 are shown in Figure 8. For H&E staining, the tumor densities were all significantly reduced by systemic administration of the prepared drugs compared with the NS group, and the areas of fibrous connective tissues simultaneously increased. Furthermore, necrosis and apoptosis of tumor cells and inflammatory cellular infiltrations were more obvious in the PTX-Lip2N group than in the other intervention groups. The cell proliferation rates were calculated by the Ki-67 index. Remarkably, the four intervention groups were all significantly lower than the control group (78.3 ± 8.75%, $p < 0.05$). PTX-Lip2N (24.2 ± 6.65%) was more effective in inhibiting tumor cells than PTX (56.7 ± 8.16%, $p < 0.001$) and PTX-Lip (43.3 ± 9.31%, $p < 0.05$), indicating that after modified by the tertiary amine derivative, Lip2N increased the accumulation of PTX in PDAC tumors and enhanced the antitumor efficacy in vivo. Consistent with tumor sizes, the PTX-Lip2N treated group showed lower Ki-67 positive rates than the nab-PTX treated group (31.7 ± 10.8%, $p = 0.178$).

Discussion

Pancreatic cancer remains one of the most lethal cancers and it is currently highlighted by its resistance to chemotherapeutic drugs, which can be attributed in part to the dense stroma that acts as a physiological barrier of the tumor tissue.[39,40] Currently, albumin-bound PTX (nab-PTX) has been widely utilized in a large number of clinical trials[41–45] in combination with gemcitabine considering its relatively high concentration of PTX by targeting the PDAC stroma and its synergistic antitumor efficacy with gemcitabine. Thus, an appropriate nano delivery system with efficient stroma-penetrating ability through the PDAC barrier is a promising direction for further studies. Based on our previous studies, the propanediamine moiety with a tertiary amine derived from pancreatic developer contrast medium, ^{123}I-HIPDM, was indicated to significantly increase pancreatic accumulation of the conjugated drugs.[23,24] The PEGylated liposome modified by a proposed new residue, N,N-dimethyl-1,3-propanediamine (Lip2N), also exhibited a notable pancreas-targeting ability in delivering agents.[29] Thus, we utilized this drug delivery system loaded with PTX (PTX-Lip2N) and carried out a further study by constructing a PDOX mouse model of PDAC to evaluate its in vivo distribution within tumor tissues and antitumor efficacy against pancreatic cancer. In the current study, PTX-Lip2N was revealed to have high drug encapsulation efficiency and significantly accumulated in PDAC tumor tissues, and its antitumor efficacy was significantly superior to that of unmodified PTX-Lip in in vivo PDOX models and even more effective than nab-PTX in restraining tumor growth, however, there was no significant difference.

The clinical formulation of PTX, which is limited by its remarkable hydrophobicity, was made with a Cremophor-EL based solution with significant adverse reactions.[46,47] In recent years, nanotechnology has offered alternative PTX

nano-formulations, such as liposomes, polymeric nanoparticles and polymeric micelles, to enhance the therapeutic effect in many malignant tumors.[48,49] Modifications to outside surface of liposomes, such as PEG derivatives,[50] acylated chitosan,[51] or protein transduction domains,[52] have been reported to enhance the antitumor efficacy by either higher blood concentrations or enhanced permeability and retention (EPR) effects. In addition, the loading efficiency and stability of PTX by cationic liposomes was reported by Monpara et al to be improved by adding cholesteryl arginine ethylester.[53] The liposomal formulation of PTX based on a prodrug synthesized by conjugating PTX with glycerophosphorylcholine (GPC) was also reported to prolong the half-life in the bloodstream with reduced adverse effects.[54] In addition to intravenous administration, the oral delivery of PTX was modified by using dual-functioning chitosan-thioglycolic PTX-loaded liposomes with significant mucus adhesion and penetration ability to enhance intestinal absorption and improve oral chemotherapy efficacy.[55] Liposomes co-modified by fructose and RGD targeting transporter, such as GLUT5 and integrin $a_vb\beta3$, were reported to have enhanced anti-proliferative abilities and efficient accumulation at the tumor site of triple-negative breast cancer.[56] In the present study, both prepared liposomes encapsulated PTX with a high encapsulation efficiency over 92% and displayed suitable particle diameter and surface charge parameters, which are thought to be directly related to the endocytosis process.[57–59] The in vitro cellular uptake of Lip2N was investigated in the BxPC-3 human PDAC cell line by confocal laser scanning microscopy and flow cytometry, and the intracellular delivery efficiency of Lip2N was superior to that of unmodified liposome (Figure 2, P=0.069), which is similar to our previous study.[29] A further tumor distribution study of Lip2N was performed in orthotopic/subcutaneous PDAC models (Figure 5), in which significant tumor accumulation of Lip2N was observed after modification by the proposed residue.

Patient-derived tumor orthotopic xenografts (PDOXs) have been reported to have the capability of reproducing the molecular microenvironment and morphological characteristics of primary tumors and have been successfully used in evaluating chemotherapeutic efficacy against PDAC.[60,61] Herein, we created PODX nude mice models to mimic the real microenvironment of PDAC tumors and evaluated the antitumor efficacy of the proposed drug delivery system. In addition, we utilized a micro PET/CT imaging system to observe the formation of pancreatic orthotopic tumors with a high intake of ^{18}F-FDG (Figure 6). This noninvasive assessment was reported to have high PDAC diagnostic accuracy[62,63] and has already been successfully used in tumor models.[64] In the present research, a high ^{18}F-FDG intake region located in the area of the mouse pancreas was observed to confirm the establishment of the PDOX models before treatment.

Epithelial tissue consists of one or more layers of closely connected cells between the plasma and basolateral membranes, and its barrier function associated with material exchange was reported to be strongly associated with the bilateral pH gradient.[65,66] HIPDM, a diamine derivative, was initially proposed as a brain perfusion imaging agent with a high-affinity for cerebral blood vessels and significantly accumulated in brain tissues[67,68] after crossing the blood-brain barrier featured a pH gradient between plasma (pH 7.4) and the brain (pH 7.0).[26] This tertiary diamine derivative was considered to be neutral and lipid soluble at high pH with an affinity for brain epithelial cells, became charged after diffusing into cells at lower interval pH and could no longer diffuse out.[67] In addition, HIPDM was recommended as a pancreas-imaging agent[21,22] for its pancreas affinity to cross the epithelial barrier between the blood and the pancreas, the BPB, with a pH gradient between plasma and the acidic pancreas (pH 6.8).[25] According to these phenomena, a series of tertiary-amine propanediamine moieties derived from HIPDM were applied in combination with some crude drugs.[23,24] After tailoring by these tertiary amine groups, the compounds exhibited higher affinities for the pancreas, from which we could suppose that the specific targeting accumulation was in part mediated by the distinct affinity between the tertiary amine and the epithelial barrier with a reduced pH gradient. In the current study, the pancreatic affinities of the liposomes were significantly increased after modification by N, N-dimethyl tertiary amino moieties, and the tumor accumulation of the modified liposomes was much greater in addition to its significant accumulation in the pancreas. After all intervention processes, the pharmacodynamic results showed a significant decrease of tumor volume after PTX-Lip2N treatment compared with normal PEGylated PTX-Lip and was slightly superior to nab-PTX.

Conclusion

A PTX-loaded liposome delivery system modified by an N, N-dimethyl tertiary amino moiety was utilized in the present research and was proven to have an efficient penetrating ability towards PDAC tumor tissue and,

consequently, showed significant in vivo antitumor efficacy in PODX nude mice models of PDAC that was slightly superior to nab-PTX. This outcome provides a promising platform with a pancreas-targeting delivery ability by encapsulating different chemotherapy drugs and enhancing their antitumor efficacy in the treatment of pancreatic cancers.

Acknowledgments

The research was supported by the Science and Technology Foundation of Sichuan Province, China (Grant No: 2018SZ0012, 2018SZ0113).

Author Contributions

Tian BL designed the study. Chen Y and Wang L carried out the majority of study. Hu J conducted the laboratory studies. Chen Y, Wang L, Huang X, Zhang Y and Wu C were in charge of the animal experiments. Chen Y, Luo S and Li PW were in charge of pharmacy experiments. Tian BL offered suggestions for this work. All authors contributed to data analysis, drafting or revising the article, gave final approval of the version to be published, and agree to be accountable for all aspects of the work. Chen Y and Wang L contributed equally and shared the co-first authorship of this article.

Disclosure

The authors report no conflicts of interest in this work.

References

1. Siegel RL, Miller KD, Jemal A. Cancer statistics, 2019. *CA Cancer J Clin*. 2019;69(1):7–34. doi:10.3322/caac.21551
2. Vincent A, Herman J, Schulick R, Hruban RH, Goggins M. Pancreatic cancer. *Lancet*. 2011;378(9791):607–620. doi:10.1016/S0140-6736(10)62307-0
3. Kamisawa T, Wood LD, Itoi T, Takaori K. Pancreatic cancer. *Lancet*. 2016;388(10039):73–85. doi:10.1016/S0140-6736(16)00141-0
4. Mayo SC, Nathan H, Cameron JL, et al. Conditional survival in patients with pancreatic ductal adenocarcinoma resected with curative intent. *Cancer*. 2012;118(10):2674–2681. doi:10.1002/cncr.26553
5. Tsai S, Erickson BA, Dua K, Ritch PS, Tolat P, Evans DB. Evolution of the management of resectable pancreatic cancer. *J Oncol Pract*. 2016;12(9):772–778. doi:10.1200/JOP.2016.015818
6. Watkins DJ, Starling N, Cunningham D, et al. The combination of a chemotherapy doublet (gemcitabine and capecitabine) with a biological doublet (bevacizumab and erlotinib) in patients with advanced pancreatic adenocarcinoma. The results of a Phase I/II study. *Eur J Cancer*. 2014;50(8):1422–1429. doi:10.1016/j.ejca.2014.02.003
7. Scagliotti GV, Parikh P, von Pawel J, et al. Phase III study comparing cisplatin plus gemcitabine with cisplatin plus pemetrexed in chemotherapy-naive patients with advanced-stage non-small-cell lung cancer. *J Clin Oncol*. 2008;26(21):3543–3551. doi:10.1200/JCO.2007.15.0375
8. Van Cutsem E, Vervenne WL, Bennouna J, et al. Phase III trial of bevacizumab in combination with gemcitabine and erlotinib in patients with metastatic pancreatic cancer. *J Clin Oncol*. 2009;27(13):2231–2237. doi:10.1200/JCO.2008.20.0238
9. Neoptolemos JP, Stocken DD, Bassi C, et al. Adjuvant chemotherapy with fluorouracil plus folinic acid vs gemcitabine following pancreatic cancer resection: a randomized controlled trial. *JAMA*. 2010;304(10):1073–1081. doi:10.1001/jama.2010.1275
10. Herrmann R, Bodoky G, Ruhstaller T, et al. Gemcitabine plus capecitabine compared with gemcitabine alone in advanced pancreatic cancer: a randomized, multicenter, phase III trial of the swiss group for clinical cancer research and the central European cooperative oncology group. *J Clin Oncol*. 2007;25(16):2212–2217. doi:10.1200/JCO.2006.09.0886
11. Conroy T, Desseigne F, Ychou M, et al. FOLFIRINOX versus gemcitabine for metastatic pancreatic cancer. *N Engl J Med*. 2011;364(19):1817–1825. doi:10.1056/NEJMoa1011923
12. Kim S, Signorovitch JE, Yang H, et al. Comparative effectiveness of nab-paclitaxel plus gemcitabine vs FOLFIRINOX in metastatic pancreatic cancer: a retrospective nationwide chart review in the United States. *Adv Ther*. 2018;35(10):1564–1577. doi:10.1007/s12325-018-0784-z
13. Gillen S, Schuster T, Meyer Zum Buschenfelde C, Friess H, Kleeff J. Preoperative/neoadjuvant therapy in pancreatic cancer: a systematic review and meta-analysis of response and resection percentages. *PLoS Med*. 2010;7(4):e1000267. doi:10.1371/journal.pmed.1000267
14. Rawla P, Sunkara T, Gaduputi V. Epidemiology of pancreatic cancer: global trends, etiology and risk factors. *World J Oncol*. 2019;10(1):10–27. doi:10.14740/wjon1166
15. Kamisawa T, Isawa T, Koike M, Tsuruta K, Okamoto A. Hematogenous metastases of pancreatic ductal carcinoma. *Pancreas*. 1995;11(4):345–349. doi:10.1097/00006676-199511000-00005
16. Ireland L, Santos A, Ahmed MS, et al. Chemoresistance in pancreatic cancer is driven by stroma-derived insulin-like growth factors. *Cancer Res*. 2016;76(23):6851–6863. doi:10.1158/0008-5472.CAN-16-1201
17. Dauer P, Nomura A, Saluja A, Banerjee S. Microenvironment in determining chemo-resistance in pancreatic cancer: neighborhood matters. *Pancreatology*. 2017;17(1):7–12. doi:10.1016/j.pan.2016.12.010
18. Olive KP, Jacobetz MA, Davidson CJ, et al. Inhibition of Hedgehog signaling enhances delivery of chemotherapy in a mouse model of pancreatic cancer. *Science*. 2009;324(5933):1457–1461. doi:10.1126/science.1171362
19. Khan S, Ebeling MC, Chauhan N, et al. Ormeloxifene suppresses desmoplasia and enhances sensitivity of gemcitabine in pancreatic cancer. *Cancer Res*. 2015;75(11):2292–2304. doi:10.1158/0008-5472.CAN-14-2397
20. Frese KK, Neesse A, Cook N, et al. nab-Paclitaxel potentiates gemcitabine activity by reducing cytidine deaminase levels in a mouse model of pancreatic cancer. *Cancer Discov*. 2012;2(3):260–269. doi:10.1158/2159-8290.CD-11-0242
21. Yamamoto K, Srivastava PS,SC, Meinken GE, Brill AB, Brill AB. Pancreas accumulation of radioiodinated HIPDM in mice and rats. *J Nucl Med*. 1985;26(7):765–769.
22. Yamamoto K, Saji TS,H, Kubo S, et al. Human pancreas scintigraphy using iodine-123-labeled HIPDM and SPECT. *J Nucl Med*. 1990;31(6):1015–1019.
23. Li J, Zhang J, Fu Y, et al. Dual pancreas- and lung-targeting therapy for local and systemic complications of acute pancreatitis mediated by a phenolic propanediamine moiety. *J Controlled Release*. 2015;212:19–29. doi:10.1016/j.jconrel.2015.06.011
24. Luo S, Li P, Li S, et al. N,N-dimethyl tertiary amino group mediated dual pancreas- and lung-targeting therapy against acute pancreatitis. *Mol Pharm*. 2017;14(5):1771–1781.

25. Behrendorff N, Floetenmeyer M, Schwiening C, Thorn P. Protons released during pancreatic acinar cell secretion acidify the lumen and contribute to pancreatitis in mice. *Gastroenterology*. 2010;139(5):1711–1720. doi:10.1053/j.gastro.2010.07.051
26. Hladky SB, Barrand MA. Fluid and ion transfer across the blood-brain and blood-cerebrospinal fluid barriers; a comparative account of mechanisms and roles. *Fluids Barriers CNS*. 2016;13(1):19.
27. Burns GP, Stein TA, Kabnick LS. Blood-pancreatic juice barrier to antibiotic excretion. *Am J Surg*. 1986;151(2):205–208. doi:10.1016/0002-9610(86)90070-X
28. Zhao Y, Liao Q, Xue C. [The effect of blood-pancreatic juice barrier on antitumor drugs excretion]. *Zhonghua Wai Ke Za Zhi*. 1997;35(5):302–304. Chinese.
29. Li PW, Luo S, Xiao LY, et al. A novel gemcitabine derivative-loaded liposome with great pancreas-targeting ability. *Acta Pharmacol Sin*. 2019;40(11):1448–1456. doi:10.1038/s41401-019-0227-7
30. Zeng YC, Li S, Liu C, et al. Soluplus micelles for improving the oral bioavailability of scopoletin and their hypouricemic effect in vivo. *Acta Pharmacol Sin*. 2017;38(3):424–433. doi:10.1038/aps.2016.126
31. Bryla A, Juzwa W, Weiss M, Lewandowicz G. Lipid nanoparticles assessment by flow cytometry. *Int J Pharm*. 2017;520(1–2):149–157. doi:10.1016/j.ijpharm.2017.01.047
32. Miao YB, Ren HX, Gan N, Cao Y, Li T, Chen Y. Fluorescent aptasensor for chloramphenicol detection using DIL-encapsulated liposome as nanotracer. *Biosens Bioelectron*. 2016;81:454–459. doi:10.1016/j.bios.2016.03.034
33. Cai W, Ratnayake R, Gerber MH, et al. Development of apratoxin S10 (Apra S10) as an anti-pancreatic cancer agent and its preliminary evaluation in an orthotopic patient-derived xenograft (PDX) model. *Invest New Drugs*. 2019;37(2):364–374. doi:10.1007/s10637-018-0647-0
34. Hiroshima Y, Maawy A, Zhang Y, et al. Metastatic recurrence in a pancreatic cancer patient derived orthotopic xenograft (PDOX) nude mouse model is inhibited by neoadjuvant chemotherapy in combination with fluorescence-guided surgery with an anti-CA 19-9-conjugated fluorophore. *PLoS One*. 2014;9(12):e114310. doi:10.1371/journal.pone.0114310
35. Hiroshima Y, Zhao M, Maawy A, et al. Efficacy of Salmonella typhimuriumA1-R versus chemotherapy on a pancreatic cancer patient-derived orthotopic xenograft (PDOX). *J Cell Biochem*. 2014;115(7):1254–1261. doi:10.1002/jcb.24769
36. Abbasi AZ, Prasad P, Cai P, et al. Manganese oxide and docetaxel co-loaded fluorescent polymer nanoparticles for dual modal imaging and chemotherapy of breast cancer. *J Controlled Release*. 2015;209:186–196. doi:10.1016/j.jconrel.2015.04.020
37. Chen K, Qian W, Jiang Z, et al. Metformin suppresses cancer initiation and progression in genetic mouse models of pancreatic cancer. *Mol Cancer*. 2017;16(1):131. doi:10.1186/s12943-017-0701-0
38. Dowsett M, Nielsen TO, A'Hern R, et al. Assessment of Ki67 in breast cancer: recommendations from the International Ki67 in Breast Cancer working group. *J Natl Cancer Inst*. 2011;103(22):1656–1664. doi:10.1093/jnci/djr393
39. Weniger M, Honselmann KC, Liss AS. The Extracellular Matrix and Pancreatic Cancer: A Complex Relationship. *Cancers (Basel)*. 2018;10(9):316. doi:10.3390/cancers10090316
40. Aroldi F, Zaniboni A. Immunotherapy for pancreatic cancer: present and future. *Immunotherapy*. 2017;9(7):607–616. doi:10.2217/imt-2016-0142
41. Von Hoff DD, Ramanathan RK, Borad MJ, et al. Gemcitabine plus nab-paclitaxel is an active regimen in patients with advanced pancreatic cancer: a phase I/II trial. *J Clin Oncol*. 2011;29(34):4548–4554. doi:10.1200/JCO.2011.36.5742
42. Goldstein D, El-Maraghi RH, Hammel P, et al. nab-Paclitaxel plus gemcitabine for metastatic pancreatic cancer: long-term survival from a phase III trial. *J Natl Cancer Inst*. 2015;107(2):dju413–dju413. doi:10.1093/jnci/dju413
43. Macarulla T, Pazo-Cid R, Guillen-Ponce C, et al. Phase I/II Trial to Evaluate the Efficacy and Safety of Nanoparticle Albumin-Bound Paclitaxel in Combination With Gemcitabine in Patients With Pancreatic Cancer and an ECOG Performance Status of 2. *J Clin Oncol*. 2019;37(3):230–238. doi:10.1200/JCO.18.00089
44. Karasic TB, O'Hara MH, Loaiza-Bonilla A, et al. Effect of Gemcitabine and nab-Paclitaxel With or Without Hydroxychloroquine on Patients With Advanced Pancreatic Cancer: A Phase 2 Randomized Clinical Trial. *JAMA Oncol*. 2019;5(7):993–998. doi:10.1001/jamaoncol.2019.0684
45. Jameson GS, Borazanci E, Babiker HM, et al. Response Rate Following Albumin-Bound Paclitaxel Plus Gemcitabine Plus Cisplatin Treatment Among Patients With Advanced Pancreatic Cancer: A Phase 1b/2 Pilot Clinical Trial. *JAMA Oncol*. 2019;6(1):125.
46. Szebeni J, Muggia FM, Alving CR. Complement activation by Cremophor EL as a possible contributor to hypersensitivity to paclitaxel: an in vitro study. *J Natl Cancer Inst*. 1998;90(4):300–306. doi:10.1093/jnci/90.4.300
47. Kloover JS, den Bakker MA, Gelderblom H, van Meerbeeck JP. Fatal outcome of a hypersensitivity reaction to paclitaxel: a critical review of premedication regimens. *Br J Cancer*. 2004;90(2):304–305. doi:10.1038/sj.bjc.6601303
48. Sofias AM, Dunne M, Storm G, Allen C. The battle of "nano" paclitaxel. *Adv Drug Deliv Rev*. 2017;122:20–30. doi:10.1016/j.addr.2017.02.003
49. Bernabeu E, Cagel M, Lagomarsino E, Moretton M, Chiappetta DA. Paclitaxel: what has been done and the challenges remain ahead. *Int J Pharm*. 2017;526(1–2):474–495. doi:10.1016/j.ijpharm.2017.05.016
50. Han SM, Baek JS, Kim MS, Hwang SJ, Cho CW. Surface modification of paclitaxel-loaded liposomes using d-alpha-tocopheryl polyethylene glycol 1000 succinate: enhanced cellular uptake and cytotoxicity in multidrug resistant breast cancer cells. *Chem Phys Lipids*. 2018;213:39–47. doi:10.1016/j.chemphyslip.2018.03.005
51. Nanda B, Manjappa AS, Chuttani K, Balasinor NH, Mishra AK, Ramachandra Murthy RS. Acylated chitosan anchored paclitaxel loaded liposomes: pharmacokinetic and biodistribution study in Ehrlich ascites tumor bearing mice. *Int J Biol Macromol*. 2019;122:367–379. doi:10.1016/j.ijbiomac.2018.10.071
52. Ju RJ, Cheng L, Xiao Y, et al. PTD modified paclitaxel anti-resistant liposomes for treatment of drug-resistant non-small cell lung cancer. *J Liposome Res*. 2018;28(3):236–248. doi:10.1080/08982104.2017.1327542
53. Monpara J, Kanthou C, Tozer GM, Vavia PR. Rational Design of Cholesterol Derivative for Improved Stability of Paclitaxel Cationic Liposomes. *Pharm Res*. 2018;35(4):90.
54. Ling L, Du Y, Ismail M, et al. Self-assembled liposomes of dual paclitaxel-phospholipid prodrug for anticancer therapy. *Int J Pharm*. 2017;526(1–2):11–22. doi:10.1016/j.ijpharm.2017.04.024
55. Liu Y, Yang T, Wei S, et al. Mucus adhesion- and penetration-enhanced liposomes for paclitaxel oral delivery. *Int J Pharm*. 2018;537(1–2):245–256. doi:10.1016/j.ijpharm.2017.12.044
56. Pu Y, Zhang H, Peng Y, et al. Dual-targeting liposomes with active recognition of GLUT5 and alphavbeta3 for triple-negative breast cancer. *Eur J Med Chem*. 2019;183:111720. doi:10.1016/j.ejmech.2019.111720
57. Roger E, Lagarce F, Garcion E, Benoit JP. Lipid nanocarriers improve paclitaxel transport throughout human intestinal epithelial cells by using vesicle-mediated transcytosis. *J Controlled Release*. 2009;140(2):174–181. doi:10.1016/j.jconrel.2009.08.010
58. Salatin S, Maleki Dizaj S, Yari Khosroushahi A. Effect of the surface modification, size, and shape on cellular uptake of nanoparticles. *Cell Biol Int*. 2015;39(8):881–890. doi:10.1002/cbin.10459

59. Kumari A, Yadav SK. Cellular interactions of therapeutically delivered nanoparticles. *Expert Opin Drug Deliv*. 2011;8(2):141–151. doi:10.1517/17425247.2011.547934
60. Vlachogiannis G, Hedayat S, Vatsiou A, et al. Patient-derived organoids model treatment response of metastatic gastrointestinal cancers. *Science*. 2018;359(6378):920–926. doi:10.1126/science.aao2774
61. Resovi A, Bani MR, Porcu L, et al. Soluble stroma-related biomarkers of pancreatic cancer. *EMBO Mol Med*. 2018;10(8). doi:10.15252/emmm.201708741
62. Ghaneh P, Hanson R, Titman A, et al. PET-PANC: multicentre prospective diagnostic accuracy and health economic analysis study of the impact of combined modality 18fluorine-2-fluoro-2-deoxy-d-glucose positron emission tomography with computed tomography scanning in the diagnosis and management of pancreatic cancer. *Health Technol Assess*. 2018;22(7):1–114. doi:10.3310/hta22070
63. Albano D, Familiari D, Gentile R, et al. Clinical and prognostic value of 18F-FDG-PET/CT in restaging of pancreatic cancer. *Nucl Med Commun*. 2018;39(8):741–746. doi:10.1097/MNM.0000000000000862
64. Mirus M, Tokalov SV, Abramyuk A, et al. Noninvasive assessment and quantification of tumor vascularization using [18F]FDG-PET/CT and CE-CT in a tumor model with modifiable angiogenesis-an animal experimental prospective cohort study. *EJNMMI Res*. 2019;9(1):55. doi:10.1186/s13550-019-0502-0
65. Hong JH, Park S, Shcheynikov N, Muallem S. Mechanism and synergism in epithelial fluid and electrolyte secretion. *Pflugers Arch*. 2014;466(8):1487–1499. doi:10.1007/s00424-013-1390-1
66. Saint-Criq V, Gray MA. Role of CFTR in epithelial physiology. *Cell Mol Life Sci*. 2017;74(1):93–115. doi:10.1007/s00018-016-2391-y
67. Kostyniak PJ. Preliminary toxicity studies on N,N,N'-trimetyl-N' (2-hydroxyl-3-methyl-5-iodobenzyl)-1,3-propanediamine (HIPDM), a new brain perfusion imaging agent. *Drug Chem Toxicol*. 1984;7(5):451–462. doi:10.3109/01480548408994212
68. Kung HF, Tramposch KM, Blau M. A new brain perfusion imaging agent: [I-123]HIPDM:N,N,N'-trimethyl-N'-[2-hydroxy-3-methyl-5-iodobenzyl]-1,3-propanedia mine. *J Nucl Med*. 1983;24(1):66–72.